Evaluation of Dialysis Membranes Using a Tortuous Pore Model

Ken-ichi Kokubo and Kiyotaka Sakai
Dept. of Chemical Engineering, Waseda University, Tokyo 169-8555, Japan

The pore-size distribution and diffusive permeability of homogeneous cellulosic dialysis membranes were measured by thermoporometry and by radioisotope and photoabsorption techniques, respectively. A tortuous pore model incorporating membrane pore-size distribution, in which tortuosity differs with pore size, can predict diffusive permeability for a wide range of solute molecular weights. The tortuosity obtained using the tortuous pore model by fitting the experimentally obtained diffusive permeability varied with molecular weight (Stokes radius). To evaluate the physical meaning of the tortuosity varied with solute Stokes radius, the tortuosity of the tortuous pore model was correlated to permeability parameters of the friction model. Tortuosity is represented by a ratio of intramembrane friction coefficients for solute and water between actual and hypothetical membrane having isodiametric pores for which the straight pore model is valid. The change in the ratio with the solute is attributable to the pore-size distribution.

Introduction

The transport phenomenon in membranes is applicable in technologies for solute separation. Improvements are desired in the performance of separation membranes in many fields, but since in many cases the conditions for membrane fabrication have not been clarified, a process of trial and error has been unavoidable. If it were possible to construct a model that would relate membrane structure to solute permeability and thereby obtain an accurate understanding of the phenomenon of solute permeation in membranes, the trial and error of membrane fabrication would be reduced, and developing dialysis membranes with sufficient performance would be possible.

A wide variety of permeability models has been proposed to provide quantitative representation of the solute transfer through dialysis membranes. One of these models is a straight pore model, in which it is assumed that the pores of the membrane are of cylindrical shape (Pappenheimer et al., 1951). In straight pore models, solutes dissolved in water are treated as particles, which are subject to higher friction resistance from water in the membrane pores than in water. The rate of diffusion of the solute in the membrane is therefore lower than that in water.

This straight pore model can explain solute permeability in membranes having straight pores that were fabricated by the track-etching method (Bean et al., 1970; Fleischer et al., 1972; Quinn et al., 1972), which was confirmed by Beck and Schultz (1972) from evaluation of solute transport through the track-etched membrane and by many subsequent studies that have been reviewed by Deen (1987). The structure of filtration and dialysis membranes, however, is considerably more complex, and application of the straight pore model to the solute permeability of these membranes may result in discrepancies between the theoretical and experimental values. This has resulted in the development of models that account for the increase in the length of the transfer path or a pore-size distribution.

Sakai et al. (1985) introduced a tortuosity for the straight pore model proposed by Verniory et al. (1973) that is obtained by exclusion of hydrodynamic resistance from a tortuous factor proposed by Mackie and Meares (1955) to account for the increased length of the solute path. This tortuous pore model makes it possible to explain the diffusive permeability of dialysis membranes for low molecular weight substances (Sakai et al., 1987, 1988). At larger molecular weights, however, the values predicted by the tortuous pore model begin to diverge from those obtained experimentally. Nakao and Kimura (1981) applied the straight pore model to the analysis

---

Correspondence concerning this article should be addressed to K. Sakai.

of data from ultrafiltration experiments, and reported that the value of the parameter $A_k/\Delta x$ in the model increased by the third power of the solute's Stokes radius. Tsapuik et al. (1990) found that effective membrane thickness decreased as molecular weight increased for cellulose acetate membranes, but the effective membrane thickness was independent of molecular weight for track-etched membranes. Unlike the straight pore model, however, this study did not account for the friction factor. Since tortuosity is not constant for a broad range of molecular weights in these studies, tortuosity alone is inadequate in explaining solute permeability in actual membranes.

Studies exist that focus on the fact that membranes have a pore-size distribution. Robertson and Zydney (1990) and Opong and Zydney (1991) studied the effect of membrane pore-size distribution on hindered diffusive permeability and the asymptotic sieving coefficient, using the effective ratio of Stokes radius to pore radius obtained by the specific volume of the pore. Mochizuki and Zydney (1993) also investigated the effect of pore-size distribution on hindered diffusive permeability, the asymptotic sieving coefficient, and the pure-water permeability. There is a problem, however, in the method of determining the pore-size distribution. Mochizuki and Zydney used a log-normal distribution, and investigated the effect of pore-size distribution on diffusive permeability assuming membranes of various distributions. Broek et al. (1992) proposed a method for evaluating the permeability of dialysis membranes using a pore-size distribution found by thermoporometry. It is not clear, however, that diffusive permeability can be explained by a discussion of pore-size distribution.

In contrast to the pore models, which are constructed hydrodynamically on the assumption that the internal structure of the membrane is geometric, the friction model (Spiegler, 1958) approaches permeability from the standpoint of nonequilibrium thermodynamics. This friction model relates intramembrane friction coefficients between solute and solvent, solute and membrane, and solvent and membrane to three transport coefficients: the pure-water permeability, the diffusive permeability, and the reflection coefficient. These friction coefficients represent interactions between the solute, solvent, and membrane during passage through the membrane. It becomes possible to clarify the physical meaning of tortuosity through these friction coefficients.

Verniory et al. (1973) established the linkage of the parameters of the friction model to those of the straight pore model, but linkage to the parameters of the tortuous pore model has not yet been achieved. The tortuosity factor proposed by Mackie and Meares (1955) has been related to the friction coefficients of the friction model, but since it includes the effects of both collisions and friction, it differs in meaning from tortuosity as used in the tortuous pore model.

If the meaning of a solute permeability model's parameters can be defined in physical terms, the model can be used to estimate diffusive permeability under a clear understanding of the limit for application of the model. It is therefore essential to clarify the meaning of tortuosity in the tortuous pore model and to establish linkage between tortuosity and the parameters of friction model.

Accordingly, in this work the pore-size distribution of cellulose dialysis membranes was measured by thermoporometry, and the diffusive permeability of the membranes was studied using a tortuous pore model that took account of pore-size distribution. In considering the effect of pore-size distribution, an investigation was made of the ways in which tortuosity varied according to the solute. Next, a tortuous pore model in which tortuosity was treated as a variable that varied with molecular weight (Stokes radius) was used to evaluate the diffusive permeability of dialysis membranes. Linkages were then established between the permeability parameters of the tortuous pore model and the friction model (Spiegler, 1958), and consideration was given to the physical meaning of tortuosity, which varied with the molecular weight (Stokes radius).

Theoretical Model

Tortuosity in the tortuous pore model

The tortuous pore model postulates that the pores twist and turn within the membrane, thus adding to the straight pore model a concept, tortuosity, that defines the ratio of pore length to membrane thickness. According to this model (Sakai et al., 1985, 1987, 1988), we can represent the diffusive permeability k_M and the pure-water permeability L_p by

$$k_M = D_w f(q) S_D \frac{A_k}{\tau \Delta x} \tag{1}$$

and

$$L_p = \frac{r_p^2 A_k}{8 \mu \tau \Delta x} \tag{2}$$

where

$$f(q) = \frac{1 - 2.1050q + 2.0865q^3 - 1.7068q^5 + 0.72603q^6}{1 - 0.75857q^5} \tag{3}$$

and

$$S_D = (1-q)^2 \tag{4}$$

Equation 3 was derived by Haberman and Sayre (1958) from the analysis of moving liquids inside cylindrical tubes with a rigid sphere.

At this time, the relationship among tortuosity τ, membrane surface porosity A_k, and water content H may be expressed by

$$H = A_k \tau \tag{5}$$

and, since the diffusive permeability is

$$k_M = \frac{K_p D_m}{\Delta x} \tag{6}$$

we see from Eqs. 1, 5, and 6 that

$$\frac{K_p D_m}{D_w} = \frac{f(q) S_D H}{\tau^2} \tag{7}$$

Here the expression

$$K_p = (1-q)^2 H \tag{8}$$

is satisfied, and the intramembrane diffusion coefficient D_m will be

$$\frac{D_m}{D_w} = \frac{f(q)}{\tau^2} \tag{9}$$

Equation 8 is not true, however, if the solute is not spherical (Giddings et al., 1968) or if there is some interaction, such as adsorption, between the solute and the membrane.

Mackie and Meares (1955) held that, in considering ion mobility, Brownian motion inside the membrane is restricted, with the result that the distance of motion increases θ-fold and driving force increases $1/\theta$-fold, so that ion mobility within the membrane would be equal to the water mobility divided by θ^2. Applying this thinking to the intramembrane diffusion coefficient they obtained

$$D_m = \frac{D_w}{\theta^2} \tag{10}$$

Mackie and Meares also derived an equation representing θ in terms of water content. The tortuosity factor θ should differ depending on solute size because collision frequency and friction are dependent on the size of the molecules.

Mackie and Meares were able to explain their experimental results by treating the tortuosity factor as a constant value that did not vary with the ion. Over a broad range of molecular weights, however, the value of θ does vary and determining intramembrane diffusion coefficient with sufficient accuracy is not possible. Eq. 9 is suitable for estimating the intramembrane diffusion coefficient over a broad range of molecular weights.

Deriving membrane structural parameters using the tortuous pore model

Canceling out $A_k/\tau\Delta x$ from Eqs. 1 and 2, we obtain

$$r_p^2 = \frac{8\mu D_w L_p}{k_M} f(q) S_D \tag{11}$$

and may then substitute the measured values of pure-water permeability L_p and diffusive permeability for tritium-labeled water (HTO) k_M to find pore radius r_p.

The water content H can be represented using membrane surface porosity and tortuosity, as shown in Eq. 5. Thus, using Eq. 5 together with the value of $A_k/\tau\Delta x$, which can be found from the measured values for L_p and k_M and the determined value for r_p, we can express membrane surface porosity A_k and tortuosity τ by

$$A_k = \sqrt{H\Delta x\left(\frac{A_k}{\tau\Delta x}\right)} \tag{12}$$

and

$$\tau = \sqrt{\frac{H}{\Delta x\left(\dfrac{A_k}{\tau\Delta x}\right)}} \tag{13}$$

It is thus possible, using the tortuous pore model, to determine pore radius r_p, membrane surface porosity A_k and tortuosity τ from water content H, the pure water permeability L_p, and the diffusive permeability for HTO k_M.

In the straight pore model, diffusive permeability for HTO and pure water permeability can be expressed as

$$k_M = D_w f(q) S_D \frac{A_k}{\Delta x} \tag{14}$$

and

$$L_p = \frac{r_p^2 A_k}{8\mu\Delta x} \tag{15}$$

Here, canceling $A_k/\Delta x$ from Eqs. 14 and 15 gives Eq. 11, so that the pore radius obtained from the tortuous pore model has the same value as that obtained by the straight pore model. Since cylindrical pores perpendicular to the surface are assumed in the straight pore model, we have

$$A_k = H \tag{16}$$

If, however, the pore radius from Eqs. 14 and 15 uses the value of water content for membrane surface porosity, the values of pore radius obtained are different. That is to say, if Eq. 16 is assumed, no pore radius exists at which both Eqs. 14 and 15 are satisfied except for membranes made by track etching.

Introducing pore-size distribution to the tortuous pore model

When pores of radius r_{pn} are present at membrane surface porosity A_k, the diffusive permeability k_{Mn} can be represented according to the tortuous pore model by

$$k_{Mn} = D_w f(q_n) S_{Dn} \frac{A_k}{\tau_n \Delta x} \tag{17}$$

The overall diffusive permeability can then be expressed by the sum of a series of values representing the diffusive permeabilities at each pore size multiplied by the ratio A_{kn}/A_k

$$k_M = \frac{A_{k1}}{A_k}k_{M1} + \frac{A_{k2}}{A_k}k_{M2} + \frac{A_{k3}}{A_k}k_{M3} + \ldots + \frac{A_{kn}}{A_k}k_{Mn} \tag{18}$$

If it is assumed that tortuosity does not vary with pore size, we obtain

$$A_k = \sum_{n=1}^{n} A_{kn} \tag{19}$$

and

$$A_{kn} = \frac{V_{pn}}{\sum_{n=1}^{n} V_{pn}} A_k = \frac{V_{pn}}{H} A_k = \frac{V_{pn}}{\tau} \tag{20}$$

If we apply the tortuous pore model to each of these pore sizes, we can substitute Eqs. 17 and 20 into Eq. 18, and the intramembrane diffusion coefficient may be expressed as

$$\frac{K_p D_w}{D_w} = \frac{\sum_{n=1}^{n} \left(f(q_n) S_{Dn} V_{pn} \right)}{\tau^2} \tag{21}$$

This is the equation proposed by Broek et al. (1992), and the change in the intramembrane diffusion coefficient due to the Stokes radius under these conditions has been reported (Kokubo et al., 1996).

For the case in which tortuosity changes with pore size, the overall intramembrane diffusion coefficient becomes

$$\frac{K_p D_w}{D_w} = \sum_{n=1}^{n} \frac{f(q_n) S_{Dn} V_{pn}}{\tau_n^2} \tag{22}$$

where

$$V_{pn} = A_{kn} \tau_n \tag{23}$$

and

$$H = \sum_{n=1}^{n} V_{pn} = \sum_{n=1}^{n} A_{kn} \tau_n \tag{24}$$

In finding the intramembrane diffusion coefficient using Eqs. 21 and 22, calculations were made for all values of pore radius r_p from 0.1 to 50 nm in 0.1-nm steps. The distribution used was log-normal, as shown in

$$n(r_{pn}) = n_0 \exp\left[- \left\{ \frac{\log(r_{pn}/R_m)}{\log \sigma_1} \right\}^2 \right] \tag{25}$$

where R_m and σ_1 were determined so as to achieve agreement with the pore-size distribution obtained by thermoporometry.

Calculating friction coefficients

The three friction coefficients in the friction model for solute to solvent, solute to membrane, and solvent to membrane were calculated by Spiegler (1958) from transport coefficients according to

$$f_{sw} = \left(S - \frac{\omega V_s}{L_p} \right) \frac{H}{\Delta x \omega} \tag{26}$$

$$f_{sm} = \left(\frac{K_p}{H} - S + \frac{\omega V_s}{L_p} \right) \frac{H}{\Delta x \omega} \tag{27}$$

and

$$f_{wm} = V_w \left[\frac{H}{\Delta x L_p} - \frac{C_s S H}{\Delta x \omega} \left(\frac{K_p}{H} - S + \frac{\omega V_s}{L_p} \right) \right] \tag{28}$$

Table 1 shows the values of the parameters used in calculating the friction coefficients. Since the solutes used were of low molecular weight, there was virtually no rejection by the membrane, making measurement of the rejection factor difficult. The value used for the asymptotic sieving coefficient S was therefore calculated by the tortuous pore model. Measured values were used for the pure-water permeability L_p, membrane thickness Δx, water content H, and diffusive permeability ω. For the V_s of vitamin B_{12}, the value used by Collins and Ramirez (1979) was adopted, and for the other solutes, V_s was calculated from the values for the solutes used by Collins and Ramirez according to regression equation

$$V_s = (1.07 MW + 0.62) \times 10^{-6} \tag{29}$$

V_w was found from the molecular weight and density of water, assuming the solution to be dilute. f_{sw}^0, which is f_{sw} in free water, was calculated from the value for the diffusion coefficient in water according to the Nernst-Einstein equation

$$f_{sw}^0 = \frac{RT}{D_w} (= 6\pi\mu r_s) \tag{30}$$

where D_w was calculated from values in the literature (Polson, 1950; Colton et al., 1971; Henderson et al., 1975; Klein et al., 1976, 1977, 1978, 1979; Wendt and Mason, 1981; Nakao

Table 1. Phenomenological Coefficients and Structural Parameters of AM-SD-M Membrane

Coefficient/Parameter	HTO	Thiourea	Nicotinamide	Tryptophan	Vitamin B_2	Vitamin B_{12}
S	0.990	0.959	0.937	0.892	0.844	0.578
ω [nmol·s·kg^{-1}·m^{-1}]	8.20	2.86	1.62	0.932	0.626	0.218
L_p [pm·s^{-1}·Pa^{-1}]	7.9	7.9	7.9	7.9	7.9	7.9
V_s [mm^3/kmol]	21.0	76.0	117	238	365	1450
V_w [mm^3/kmol]	18.1	18.1	18.1	18.1	18.1	18.1
H	0.587	0.587	0.587	0.587	0.587	0.587
Δx [μm]	23.7	23.7	23.7	23.7	23.7	23.7
C_s [mmol·m^{-3}]	0.500	0.500	0.500	0.500	0.500	0.500
f_{sw}^0 [pg·mol^{-1}·s^{-1}]	0.87	1.77	2.17	2.93	3.56	5.82

Table 2. Technical Data on Regenerated Cellulose Hollow-Fiber Dialysis Membranes

Type of Memb.	Material	ID (Wet) [μm]	Wall Thick. (Wet) [μm]	Water Content [%]	Pure-Water Permeab. [$mL \cdot m^{-2} \cdot h^{-1} \cdot mm\ Hg^{-1}$]
AM-SD-M	Regenerated cellulose	188	24	59	3.8
AM-FP	Regenerated cellulose	195	31	73	11.6

Table 3. Molecular Weight and Stokes Radius of Test Solutes

Solute	Molec. Wt.	Stokes Radius [nm]	Diffusion Coeff. [$\mu m^2/s$]
Tritium-labeled water	19	0.107	2970
Urea	61	0.182	1840
Thiourea	76	0.221	1460
Nicotinamide	121	0.276	1190
Tryptophan	204	0.372	880
Vitamin B_2	376	0.456	725
Vitamin B_{12}	1,355	0.836	443

and Kimura, 1982) using the regression equation

$$D_w = 9.0 \times 10^{-5} MW^{-0.44} \tag{31}$$

and

$$r_s = 3.1 \times 10^{-9} MW^{-0.46} \tag{32}$$

Experimental Procedures

The hollow-fiber membranes tested in these experiments were AM-SD-M and AM-FP regenerated cellulose membranes (Asahi Medical, Tokyo). Table 2 shows technical data. These membranes are normally used as dialysis membranes, are of homogeneous structure, and have a low level of pure-water permeability and of diffusive permeability to high molecular weight solutes. The solutes used in the experiments were HTO, thiourea, nicotinamide, tryptophan, and vitamins B_2 and B_{12}. Table 3 shows the molecular weight, Stokes radius, and diffusion coefficient in water of these solutes. The solvent was a phosphate buffer solution of pH 7.4.

Diffusive permeability was measured at 310 K by means of a radioisotope technique (Sakai et al., 1987, 1988) in the case of HTO, and by means of a photoabsorption technique using optical fibers (Ohmura et al., 1989; Kanamori et al., 1994) in the case of the other solutes. Both of these methods are free from the influence of solute transfer due to convection and make it possible to measure permeability due solely to diffusion. Figure 1 shows the experimental apparatus.

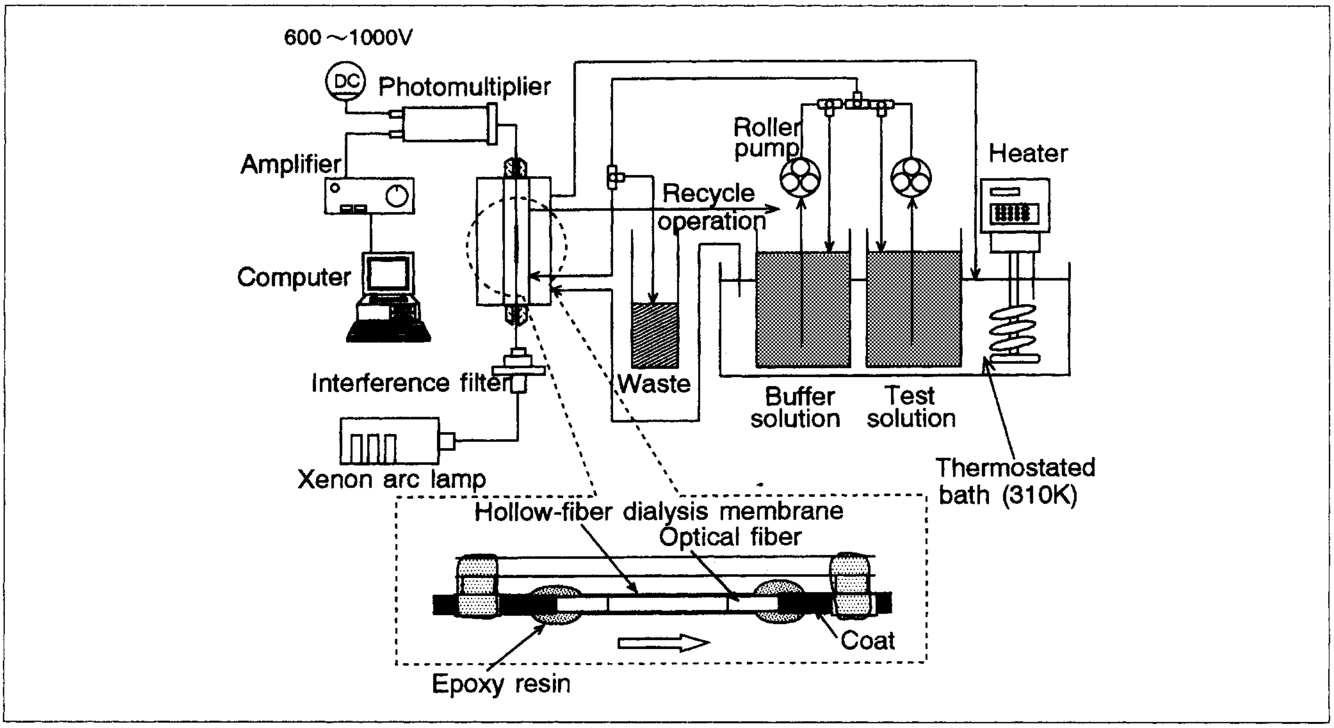

Figure 1. Apparatus for photoabsorptive measurement of diffusive permeability with dialysis membrane.
Hollow-fiber membrane with optical fibers inserted into either end.

The tips of optical fibers were inserted into either end of the hollow fiber and fixed with epoxy resin. The assembly was then mounted in a cylindrical dialyzer cell 8 mm in diameter, and all air was removed from inside the hollow fiber by means of a flow of fully degassed dialysate (isotonic phosphate buffer solution, pH 7.4). The dialyzer cell was then supplied alternately with flows of each of the test solutes (i.e., a phosphate buffered solution of each of the solutes) and the dialysate using the rate of flow (500 mL/min) at which no boundary film formation occurred. Changes in solute concentration over time were found by measuring a transmittance inside the hollow fibers. From these data, an intramembrane diffusion coefficient was calculated by the method for analyzing nonsteady state diffusion in a single hollow-fiber membrane (Stevenson, 1974).

Pore-size distribution was found by differential scanning calorimetry (DSC). Hollow-fiber membranes, which were thoroughly wetted with degassed reverse osmosis (RO) water, were cut in lengths of approximately 2 mm and were placed in a sealed aluminum sample pan after removal of excess water. The sealed pan containing the samples and an empty reference pan were placed on the sample stand of the calorimeter and were cooled to 223 K using liquid nitrogen. The temperature was then raised by 0.5 K/min heating and a thermogram was obtained.

Pore-size distribution was then calculated using the method proposed by Ishikiriyama et al. (1986), in which the pore-size distribution of polymethyl methacrylate (PMMA) membranes was measured by thermoporometry.

By combining Laplace's equation, which defines the conditions of dynamic equilibrium, with the Gibbs-Duhem equation, which defines the conditions of thermodynamic equilibrium, Brun et al. (1977) and Homshaw (1981) derived Eq. 33, in which the relationship between ΔT [K] and r_p [nm] is expressed as

$$\Delta T = \frac{2\gamma V_w T_0 \cos\alpha}{r_p \Delta H_m} = \frac{33.4}{r_p} \tag{33}$$

where the value used for the melting temperature of the bulk water T_0 (270.55 K) is obtained from the thermogram of RO water. The other values used were 18.02 m^3/Mmol for the molar volume of water V_w, 6.01 kJ/mol for the molar melting enthalpy of water ΔH_m, 0.02 N/m (Ishikiriyama et al., 1995) for the boundary tension between ice and water γ and 0 rad for the contact angle α.

The abscissa of the thermogram, representing temperature, may be converted into the pore radius using Eq. 33, and the ordinate of the thermogram, representing the rate of heat transfer dQ/dt, may then be converted into pore volume dV/dr by

$$\frac{dV_p}{dr_p} = \frac{1}{\phi L(r_p) A} (\Delta T)^2 \frac{dQ}{dt} \tag{34}$$

where A is $2\gamma V_m T_0 \cos\alpha/\Delta H_m$ (= 33.4 nm·K), $L(r_p)$ is latent heat of melting per unit volume [J/mL], V_p is the specific volume [mL/g] of pores having a radius of $0 - r_p$ [nm], and ϕ is the rate of temperature rise [K/min].

$L(r_p)$ may then be expressed as

$$L(r_p) = \frac{\Delta H_m MW}{\rho} \tag{35}$$

where, since molecular weight MW is constant (= 18), calculation becomes possible if ρ and ΔH_m are expressed as functions of T.

Since, in the equation

$$\Delta H_m = \Delta H_m(T_0) + \int_{T_0}^{T} \left[C_{p,\text{water}}(T) - C_{p,\text{ice}}(T) \right] dT \tag{36}$$

used by Ishikiriyama (1986) to represent the temperature dependence of ΔH_m, temperature dependence is extremely small, the calculation was made with $L(r_p)$ held constant.

Results and Discussion

Tortuous pore model taking account of pore-size distribution

Expressing the intramembrane diffusion coefficient as $K_p D_m/D_w$ (equal to D_{eff}/D_w), it was found to correlate with the Stokes radius r_s of the solute. Figure 2i shows a comparison of measured values of $K_p D_m/D_w$ for AM-SD-M and AM-FP membranes against the theoretical values obtained from the tortuous pore model assuming that membranes have isodiametric pores. Figure 2ii shows the tortuosity calculated using Eq. 7 from the pore radii obtained from the intramembrane diffusion coefficient of HTO and pure-water permeability, measured values of $K_p D_m/D_w$, membrane thickness (when wet), and water content. Tortuosity varied with the Stokes radius of the solute.

For membranes with a pore-size distribution, the surface porosity differs according to the solute so that there are pores that permit the passage of smaller solutes but not of larger solutes. The effect of changes in membrane surface porosity on the intramembrane diffusion coefficient was evaluated accordingly using the pore-size distribution found by thermoporometry.

Figure 3i shows the values of $K_p D_m/D_w$ obtained by the tortuous pore model for membranes having a pore-size distribution (Figure 3ii), for which we used the distribution obtained by thermoporometry and the log-normal distribution that most closely agreed with it. Table 4 shows the parameters of the log-normal distribution function. The theoretical values of $K_p D_m/D_w$ calculated from the model accounting for pore-size distribution and from the model assuming isodiametric pores were virtually identical. This can be attributed to the fact that, at the pore-size distribution obtained by thermoporometry, few pores were smaller than 1 nm, so the size of the pores permeable to the solute was about the same in both models. Figure 4 shows the values of tortuosity with and without pore size distribution. In both cases tortuosity varied with the Stokes radius.

Tortuous pore model taking account of change in tortuosity with pore size

The difference in tortuosity depending on the solute can be expressed by assuming, as shown in Figure 5, that the pores

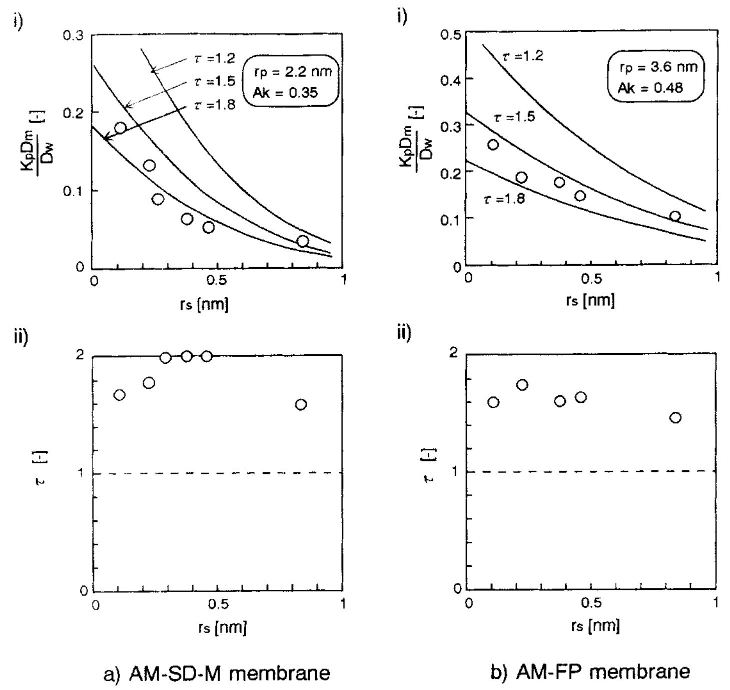

a) AM-SD-M membrane

b) AM-FP membrane

Figure 2. Stokes radius dependence of: (i) K_pD_m/D_w; (ii) tortuosity.

Solid lines show theoretical relationships calculated by the tortuous pore model for membrane with isodiametric pores.

have a branching structure, so that the smaller the pore the longer the path along which intramembrane diffusion takes place. The smaller solute is capable of also taking the smaller and more tortuous path. The tortuosity, however, should be essentially independent of solute molecular weight if it is a geometric parameter that one can use to specify the membrane structure.

Changes in tortuosity with solute size correspond to a model in which, for membranes having a pore-size distribution, tortuosity varies with pore size. When a solute passes through membrane having a tortuosity that differs with pore size, as shown in Figure 6, the pores through which transfer occurs will differ with the solute so that the value of tortuosity will vary with the size of the solute.

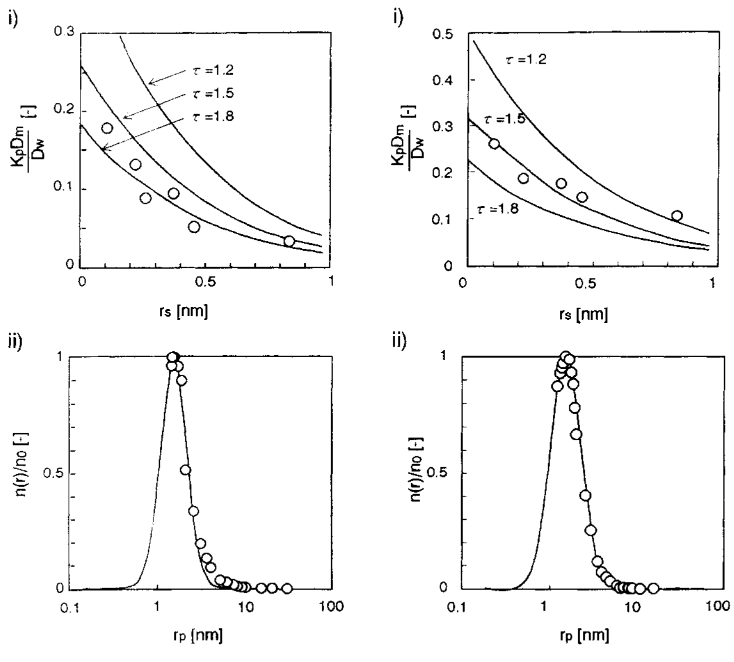

a) AM-SD-M membrane

b) AM-FP membrane

Figure 3. Stokes radius dependence of K_pD_m/D_w (i).

Solid lines show theoretical relationships calculated by the tortuous pore model for membrane having pore-size distribution shown in (ii).

Table 4. Parameters of Log-Normal Distribution Function

	Rm [nm]	n_0	σ_1
AM-SD-M	1.50	5.17×10^{22}	1.65
AM-FP	1.53	8.69×10^{22}	1.77

A calculation was thus made of the Stokes radius dependence of the intramembrane diffusion coefficient, assuming the case shown in Figure 6, in which the smaller the pore size the greater the tortuosity. An example is shown by the solid line in Figure 7, while the theoretical curves for the case in which tortuosity is constant (Figure 3) are shown by broken lines. The theoretical values determined based on changes in tortuosity with pore size (the solid lines) agree with the experimentally obtained values better than the theoretical values determined by assuming constant tortuosity irrespective of pore size (the broken lines). Thus it can be seen that, in the tortuous pore model, it is possible to find the diffusive permeability for a broad range of molecular weights if the pore size distribution is taken into account and different tortuosities are fixed depending on the pore size.

Tortuous pore model taking account of change in tortuosity with Stokes radius but not of pore-size distribution

An investigation of changes in tortuosity with membrane surface porosity was conducted at isodiametric pore size. The value used here for pore size was that obtained from the diffusive permeability of HTO, the smallest of the solutes, and tortuosity was found by substituting the measured values of K_pD_m/D_w into Eq. 7. Membrane surface porosity was found from tortuosity and water content using Eq. 5. Table 5 shows the structural parameters obtained; the values for tortuosity are identical with those shown in Fig. 2a. It is evident that the tortuosity and membrane surface porosity are solute-dependent when pore size is held constant.

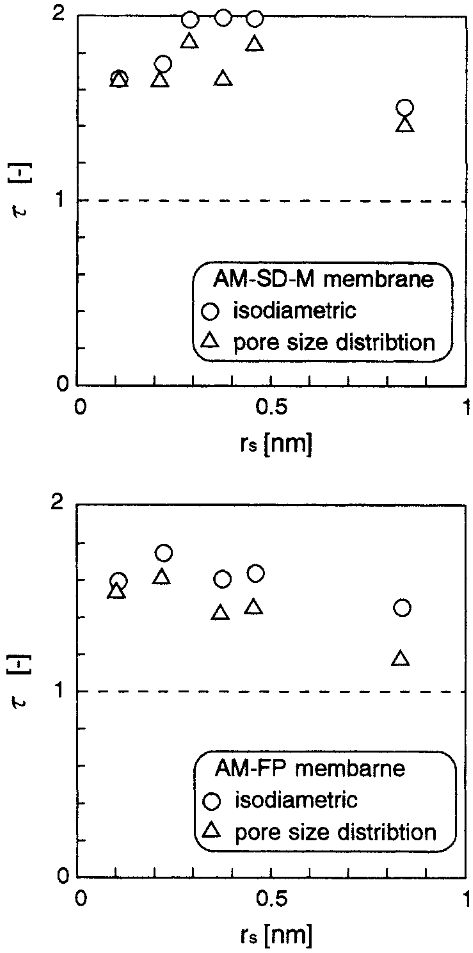

Figure 4. Calculated Stokes radius dependence of tortuosity for membrane with isodiametric pores vs. membrane with pore-size distribution measured by DSC.

A comparison was made between measured values and values calculated from the tortuous pore model, in which pore size was held constant and tortuosity varied with Stokes radius, with Figure 8. Here, in calculating the value of D_m/D_w from measured values of K_pD_m/D_w, the value of membrane partition coefficient K_p obtained from $H(1-q)^2$ was used. Using the conventional tortuous pore model, in which tortuosity is constant, the theoretical and measured values agreed

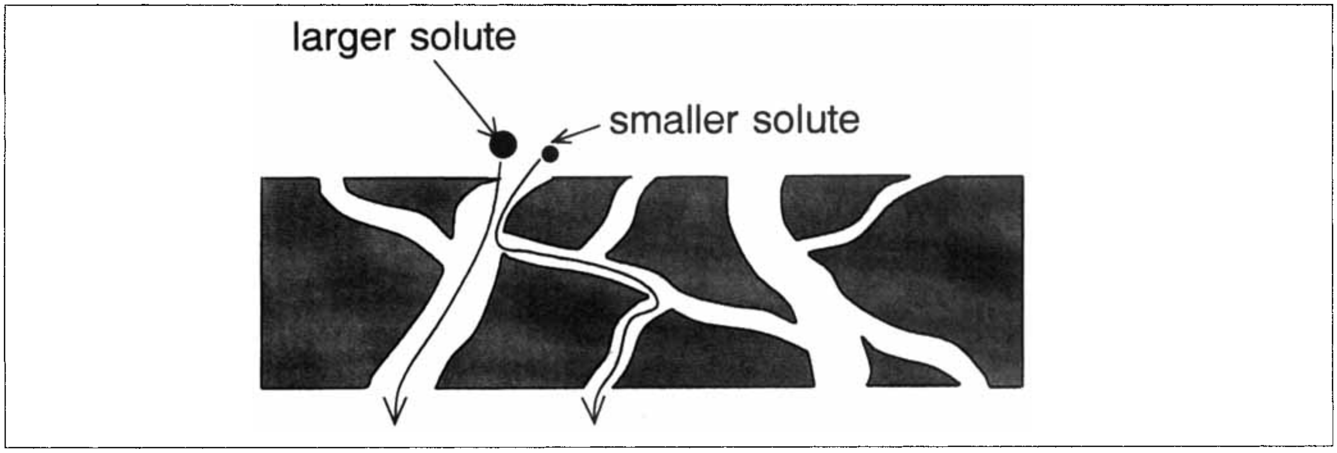

Figure 5. Molecules traversing a membrane via different paths.

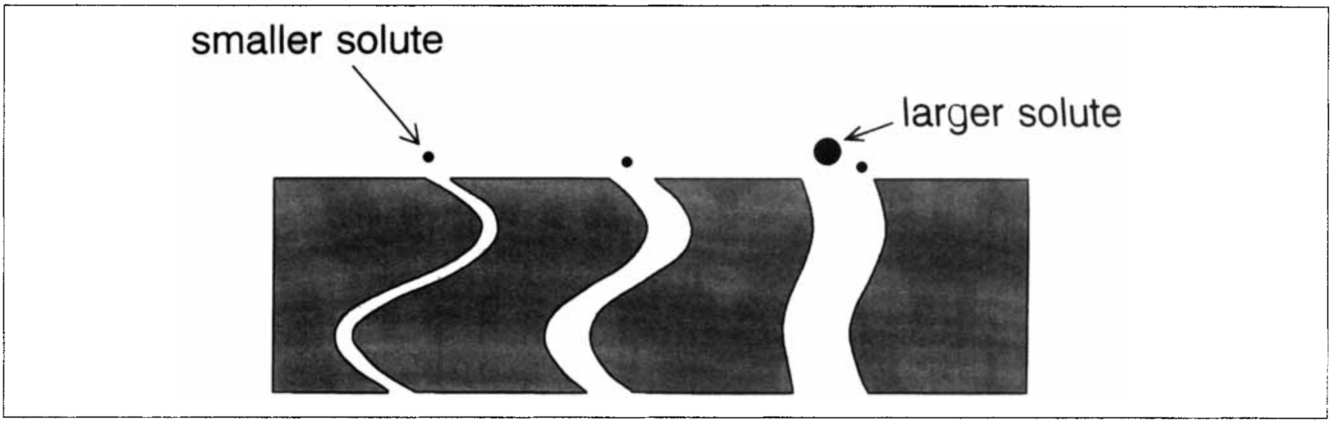

Figure 6. Molecules traversing a membrane via pores of different sizes.

for HTO, but differed for the other solutes. When tortuosity was a variable in the tortuous pore model, on the other hand, the theoretical values also agreed with the measured values for D_m/D_w (the plot ○). In this case tortuosity is an imaginative parameter for fitting the experimental data. We can discuss the physical meaning of tortuosity varying with solute molecular weight and also the difference between the experimental results and theoretical prediction from the model taking account of tortuosity varying with pore size.

When the Stokes radius of the solute is particularly small and the membrane pore size particularly large, solute diffusion approaches the diffusion through a water membrane, so that D_m/D_w becomes unity. In the tortuous pore model, however, if we consider tortuosity as a constant, $f(q)/\tau^2$, which corresponds to D_m/D_w, will be $1/\tau^2$ and will not become unity, even when the Stokes radius of the solute is extremely small. In Figure 2a, if tortuosity is considered as a variable, it can be extrapolated to unity when Stokes radius is zero so that, when the Stokes radius of a solute is extremely small, $f(q)/\tau^2$ becomes unity and $D_m = D_w$. From this viewpoint, taking tortuosity as a variable provides a more accurate description of the membrane permeability of solutes.

Comparison between the tortuous pore model and the friction model

In examining the meaning of the dependence of tortuosity on the Stokes radius of the solute, a comparison was made between the parameters of the tortuous pore model and the friction model. From Eqs. 26, 27 and 30, we may obtain

$$\frac{f_{sw}^0}{f_{sw} + f_{sm}} = \frac{D_m}{D_w} \tag{37}$$

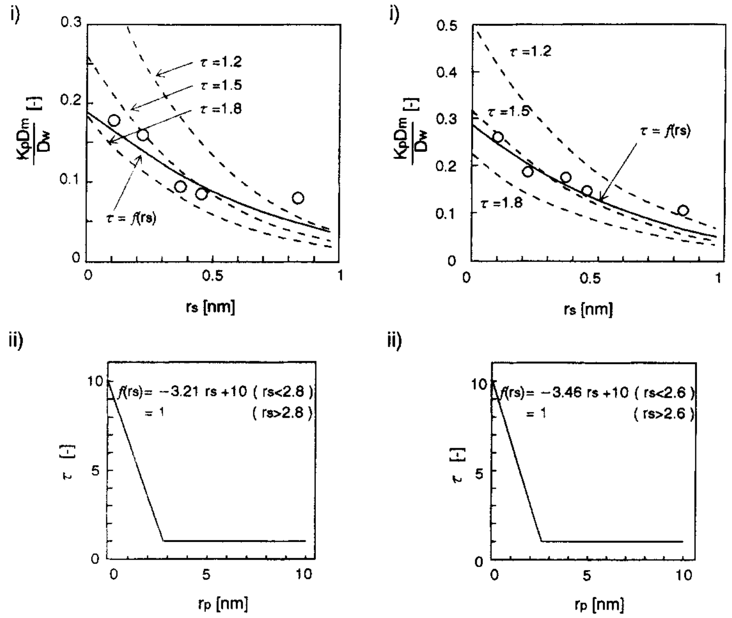

a) AM-SD-M membrane

b) AM-FP membrane

Figure 7. (i) Stokes radius dependence of K_pD_m/D_w; (ii) theoretical relationships (—) for a membrane assuming different tortuosities for each pore radius.

Calculated by the tortuous pore model.

Table 5. Structural Parameters of AM-SD-M Membrane Obtained from Tortuous Pore Model

	HTO	Thiourea	Nicotinamide	Tryptophan	VB_2	VB_{12}
r_p [nm]	2.25	2.25	2.25	2.25	2.25	2.25
Ak	0.349	0.330	0.292	0.287	0.288	0.376
τ	1.68	1.78	2.01	2.04	2.03	1.56

According to Verniory et al. (1973), the parameters of the straight pore model and the friction model can be related by

$$\frac{f_{sw}^0}{f_{sw}+f_{sm}}=f(q) \tag{38}$$

whereas, in the tortuous pore model, we have, from Eqs. 9 and 37

$$\frac{f_{sw}^0}{f_{sw}+f_{sm}}=\frac{f(q)}{\tau^2} \tag{39}$$

The values of $f(q)/\tau^2$, $f_{sw}^0/(f_{sw}+f_{sm})$ and f_{sw}^0/f_{sw} were compared (Figure 9). D_m/D_w was calculated from K_pD_m/D_w, using $K_p=\mathrm{H}(1-q)^2$; $f_{sw}^0/(f_{sw}+f_{sm})$ was calculated using measured values for ω and L_p, and $\mathrm{H}(1-q)^2$ for K_p; and f_{sw}^0/f_{sw} was calculated using measured values for ω and L_p. Values for D_m/D_w (the plot ○) agreed with $f_{sw}^0/(f_{sw}+f_{sm})$ and $f(q)/\tau^2$, and the values of f_{sw}^0/f_{sw} closely approximated to $f(q)/\tau^2$.

The parameters of the tortuous pore and friction models are related as shown in Eq. 39. In order to represent tortuosity by friction coefficients, it is necessary to know what the relationship is between $f(q)$ in Eq. 39 and the friction coefficients. Since the straight pore model does not hold true for AM-SD membranes, Eq. 38 is not satisfied. Accordingly, the diffusive permeability and the pure-water permeability were calculated for a hypothetical membrane having pore size, membrane thickness, and water content equal to an actual membrane yet satisfying the straight pore model. A comparison was then made between the friction coefficients calculated from these values and $f(q)$. The diffusive permeability and pure-water permeability of this hypothetical membrane were calculated using Eqs. 14 and 15, taking the water content for A_k, measured values for membrane thickness, 2.25 nm for pore radius, and $\mathrm{H}(1-q)^2$ for K_p. The friction coefficients were also calculated.

Figure 10 shows a comparison of the values of $f_{sw}^0/(f_{sw}+f_{sm})$ and f_{sw}^0/f_{sw} with $f(q)$ as well as friction coefficients obtained from measured values of diffusive permeability and the pure-water permeability. The value of $f_{sw}^0/(f_{sw}+f_{sm})$ obtained from measured values differed from $f(q)$, whereas the value of $f_{sw}^0/(f_{sw}+f_{sm})$ obtained from the diffusive permeability, the pure-water permeability, and partition coefficient of a hypothetical membrane in which pores were assumed to be perfectly cylindrical agreed with $f(q)$. Moreover, the value of f_{sw}^0/f_{sw} was close to that of $f(q)$.

Evaluation of tortuosity using the friction model

As we can see from Figure 9, $f(q)/\tau^2$ may be represented using the friction coefficients obtained from the diffusive permeability, pure-water permeability and membrane partition coefficient of the tortuous pore model, by

$$\frac{f(q)}{\tau^2}=\left(\frac{f_{sw}^0}{f_{sw}+f_{sm}}\right)_{t\text{-pore}} \tag{40}$$

It is also possible, as shown in Figure 10, to represent $f(q)$ using the friction coefficients calculated from the diffusive permeability, pure-water permeability, and membrane partition coefficient of a hypothetical membrane that has isodia-

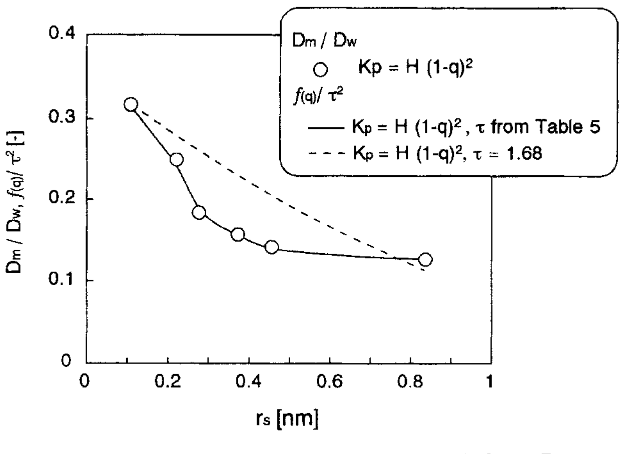

Figure 8. Stokes radius dependence of D_m/D_w and $f(q)/\tau^2$.

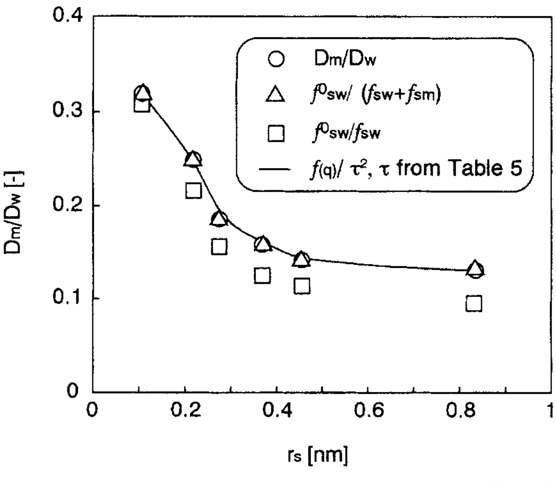

Figure 9. Stokes radius dependence of D_m/D_w, $f_{sw}^0/(f_{sw}+f_{sm})$, f_{sw}^0/f_{sw} and $f(q)/\tau^2$.

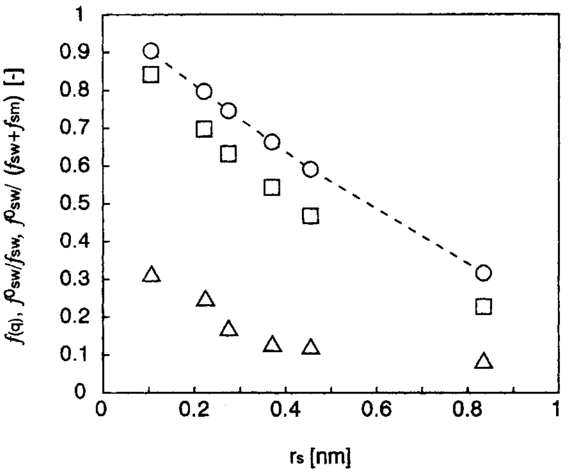

Figure 10. Stokes radius dependence of friction coefficients.

--- = friction factor $f(q)$; ○ = coefficient $f_{sw}^0/(f_{sw}+f_{sm})$, calculated from data on ω and L_p determined by straight pore model, and from $K_p = H(1-q)^2$; □ = coefficient f_{sw}^0/f_{sw}, calculated from data on ω and L_p determined by straight pore model; △ = coefficient $f_{sw}^0/(f_{sw}+f_{sm})$, calculated from data on measured values of ω and L_p, and from $K_p = H\ (1-q)^2$.

metric pore size, membrane thickness and water content, thereby satisfying the straight pore model, by

$$f(q) = \left(\frac{f_{sw}^0}{f_{sw}+f_{sm}}\right)_{s\text{-pore}} \tag{41}$$

From this, tortuosity may be given as

$$\tau^2 = \frac{(f_{sw}+f_{sm})_{t\text{-pore}}}{(f_{sw}+f_{sm})_{s\text{-pore}}} \tag{42}$$

where $f(q)/\tau^2$ and $f(q)$ have values close to those of $(f_{sw}^0/f_{sw})_{t\text{-pore}}$ and $(f_{sw}^0/f_{sw})_{s\text{-pore}}$ respectively. Here, we confirmed whether or not tortuosity could be represented by

$$\tau^2 = \frac{(f_{sw})_{t\text{-pore}}}{(f_{sw})_{s\text{-pore}}} \tag{43}$$

Figure 11 shows a comparison between the values for τ obtained from Eq. 43 and those calculated for actual solutes using the tortuous pore model (the values in Table 5); the values were found to be in good agreement. The fact that Eq. 43 held good here is attributable to the fact that f_{sm} was much smaller than f_{sw} in the membranes used, so the tortuosity value changed primarily with friction coefficient for the solute and water f_{sw}.

Mackie and Meares (1955), in their work on the ion permeability of ion-exchange membranes, compared the square of the tortuosity factor θ with f_{sw}/f_{sw}^0, demonstrating that the two were in agreement

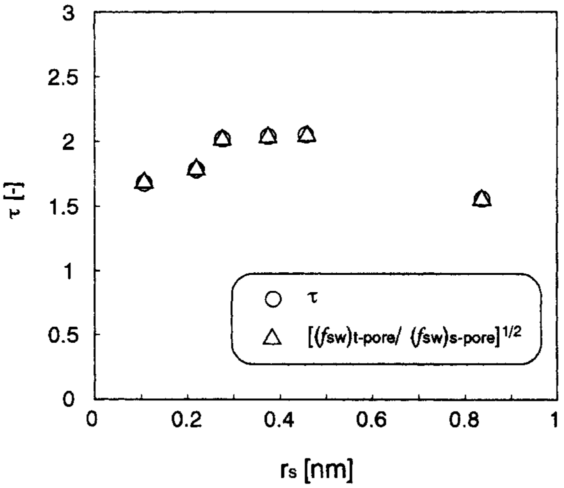

Figure 11. Stokes radius dependence of tortuosity.

$$\theta^2 = \frac{f_{sw}}{f_{sw}^0} \tag{44}$$

In the results of Kaufmann et al. (1968) and Collins et al. (1979), however, in which the permeability of dialysis membranes was evaluated by means of a friction model, the value of θ in Eq. 44 was not constant. In the results of Kaufmann et al., the value of f_{sw}/f_{sw}^0 increased with solute size, while in the results of Collins et al., f_{sw}/f_{sw}^0 varied with the solute, with the average value agreeing with θ for Cuprophan membranes, but not for PAN membranes. The data for Cuprophan membranes showed that f_{sw}/f_{sw}^0 increased with solute size, with certain exceptions. Based on Eqs. 9 and 10, the relationship between tortuosity in the tortuous pore model and the tortuosity factor of Mackie and Meares may be written as

$$\theta^2 = \frac{\tau^2}{f(q)} \tag{45}$$

Since the value of $f(q)$ is substantially constant for the ions studied by Mackie and Meares (1955), there was no solute-dependent change in θ (or in f_{sw}/f_{sw}^0), but for solutes having larger molecules, such as those studied by Kaufmann et al. and Collins et al., θ increased with molecular weight. Thus Mackie and Meares' tortuosity factor is a value that changes primarily under the influence of hydrodynamic resistance, equivalent to $f(q)$ in the tortuous pore model. Tortuosity in the tortuous pore model, on the other hand, is influenced by the other factors, and thus the tendency to change with molecular weight is clearly different from the case studied by Mackie and Meares.

One factor that may be adduced as showing the dependence of tortuosity on molecular weight (Stokes radius) in a tortuous pore model having tortuosity as a variable is that pore-size distribution is not accounted for. The Stokes radius dependence of tortuosity, however, was similar even when a pore-size distribution obtained by thermoporometry was used.

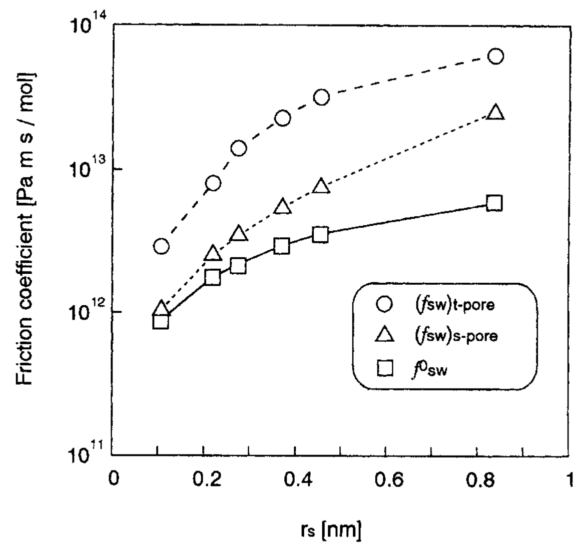

Figure 12. Stokes radius dependence of friction coefficients.

We may therefore say that changes in surface porosity have little effect for the membranes used in the present study.

As solute adsorption occurs, tortuosity differs with the solute in cases in which the interaction between the solute and membrane is large. With the membranes used in the present study, however, f_{sm} was small relative to f_{sw}, and the influence of adsorption was minor. It is therefore suggested that the cause lies in the facts that in actual membranes, pores do not have cylindrical cross-sections, but rather have branched structures, and are tortuous. To confirm this, the Stokes radius dependence of the various friction coefficients that determine tortuosity was examined (Figure 12), in which the difference between the plots of the Δ and ○ points corresponds to the change in τ dependent on the Stokes radius in Eq. 43. It was confirmed that for both large and small solutes, tortuosity was smaller. Where the solute was smaller, both $(f_{sw})_{s\text{-pore}}$ and $(f_{sw})_{t\text{-pore}}$ showed only a small difference from f_{sw}^0, and it is suggested that this small difference is due to the fact that the influence of the pore walls on f_{sw} is less. Consequently the difference between $(f_{sw})_{s\text{-pore}}$ and $(f_{sw})_{t\text{-pore}}$ is less and tortuosity is smaller.

When the solute was large, $(f_{sw})_{t\text{-pore}}$ was not as large as $(f_{sw})_{s\text{-pore}}$ predicted for the straight pore model, and accordingly tortuosity was less. The reasons for this are a) as the solute size increases the number of pores through which the solute can pass is reduced, leading to a tendency to take the less tortuous transfer path; and b) the apparent average pore size is larger and $f(q)$ is smaller. Thus if we consider that the pores are tortuous and having a branching structure with pore-size distribution, the Stokes radius dependency of tortuosity can be explained.

The tortuous pore model is valid for homogeneous membranes and for solutes of which the interaction with membrane occurs by hydrodynamic force. Eq. 43 is then valid and tortuosity is a geometric parameter of which the physical meaning is the ratio of intramembrane friction coefficients for solute and water between actual membrane and hypothetical membrane having isodiametric straight pores. Solute Stokes radius dependence of tortuosity results from membrane structure.

Conclusions

The tortuous pore model can explain the diffusive permeability of regenerated cellulose membranes having a homogeneous structure for a wide range of molecular weights by taking account of pore-size distribution and assuming a membrane structure in which tortuosity differs with pore size.

Intramembrane diffusion coefficients estimated by the tortuous pore model, in which membranes having isodiametric pores and tortuosity varies with the Stokes radius of the solute, agree with the measured values. Tortuosity is represented by a comparison of intramembrane friction coefficients for solute and water between actual membrane and hypothetical membrane having isodiametric pores for which the straight pore model is valid. The Stokes radius dependence of tortuosity results from the change in the ratio of the intramembrane friction coefficients and characterizes the membrane structure.

Acknowledgment

The authors appreciate Masahiro Taguchi and Teppei Usami for their assistance in obtaining experimental data.

Notation

C_s = solute concentration, mol/m^3
D_{eff} = effective intramembrane diffusion coefficient, m^2/s
f_{sw} = friction coefficient between solute and water, Pa·m·s/mol
f_{sm} = friction coefficient between solute and membrane, Pa·m·s/mol
f_{wm} = friction coefficient between water and membrane, Pa·m·s/mol
$f(q)$ = friction factor between inner wall of pore and solute in straight and tortuous pore model
J_s = solute flux, mol/m^{2}s
K_p = membrane partition coefficient
q = solute-to-pore size ratio, r_s/r_p
R = gas law constant, Kg·m^2·s^{-2}·mol^{-1}·K^{-1}
R_m = pore radius at the maximum in the distribution function, m
S = asymptotic sieving coefficient ($= 1 - \sigma$)
S_D = steric hindrance factor due to diffusion in straight and tortuous pore model
T = temperature, K
T_0 = melting point of bulk water, K
v_s = solute transfer rate, m/s
V_s = partial molar volume of solute, m^3/mol
V_w = partial molar volume of water, m^3/mol
α = contact angle, rad
γ = interfacial tension between ice and water, N/m
ΔH_m = molar melting enthalpy of water, J/mol
ΔT = drop in melting point, K
Δx = membrane thickness, m
ϵ = void of membrane
μ = viscosity, Pa·s
ρ = density, kg/m^3
σ = Staverman's reflection coefficient
σ_1 = geometric standard deviation
ϕ = temperature rise rate, K/s
ω = diffusive permeability ($= k_M/RT$), mol·s/(kg·m)

Literature Cited

Bean, C. P., M. V. Doyle, and G. Entine, "Etching of Submicron Pores in Irradiated Mica," *J. Appl. Phys.*, **41**, 1454 (1970).
Beck, R. E., and J. S. Schultz, "Hindrance of Solute Diffusion within

Membranes as Measured with Microporous Membranes of Known Pore Geometry," *Biochim. Biophys. Acta*, **255**, 273 (1972).

Broek, A. P., H. A. Teunis, D. Bargeman, E. D. Sprengers, and C. S. Smolders, "Characterization of Hollow Fiber Hemodialysis Membrane: Pore Size Distribution and Performance," *J. Memb. Sci.*, **73**, 143 (1992).

Brun, M., A. Lallemand, and J. F. Quinson, "A New Method for the Simultaneous Determination of the Size and the Shape of Pores: The Thermoporometry," *Thermochim. Acta*, **21**, 59 (1977).

Collins, M. C., and F. W. Ramirez, "Mass Transport Through Polymeric Membranes," *J. Phys. Chem.*, **83**, 2294 (1979).

Colton, C. K., K. A. Smith, E. W. Merrill, and P. C. Farrell, "Permeability Studies with Cellulosic Membranes," *J. Biomed. Mater. Res.*, **5**, 459 (1971).

Deen, W. M., "Hindered Transport of Large Molecules in Liquid-Filled Pores," *AIChE J.*, **33**, 1409 (1987).

Fleischer, R. L., H. W. Alter, P. B. Furman, and R. M. Walker, "Particle Track Etching," *Science*, **178**, 255 (1972).

Giddings, J. C., E. Kucera, C. P. Russell, and M. N. Myers, "Statistical Theory for the Equilibrium Distribution of Rigid Molecules in Inert Porous Networks. Exclusion Chromatography," *J. Phys. Chem.*, **72**, 4397 (1968).

Haberman, W. L., and R. M. Sayre, "Motion of Rigid and Fluid Spheres in Stationary and Moving Liquids Inside Cylindrical Tubes," David Taylor Model Basin, Hydromechanics Lab. Res. and Dev., Report No. 1143 (1958).

Henderson, L. W., M. E. Silverstein, C. A. Ford and M. J. Lysaght, "Clinical Response to Maintenance Hemodiafiltration," *Kidney Int.*, 7, S58 (1975).

Homshaw, L. G., "Calorimetric Determination of Porosity and Pore Size Distribution (PSD): Effect of Heat on Porosity, Pore Form, and PSD in Water-Saturated Polyacrylonitrile Fibers," *J. Coll. Interf. Sci.*, **84**, 127 (1981).

Ishikiriyama, K., M. Todoki, T. Kobayashi, T. Takeyama, and H. Tanzawa, "Structure of PMMA Membrane for Artificial Kidney (Ii) Pore Size Distribution in PMMA Hydrogel by Differential Scanning Calorimetry," *Polymer Preprints Jpn.*, **35**, 2090 (1986).

Ishikiriyama, K., and M. Todoki, "Pore Size Distribution (PSD) Measurements of Silica Gels by Means of Differential Scanning Calorimetry: II. Thermoporosimetry," *J. Coll. Interf. Sci.*, **171**, 92 (1995).

Kanamori, T., K. Sakai, T. Awaka, and M. Fukuda, "An Improvement on the Method of Determining the Solute Permeability of Hollow-Fiber Dialysis Membranes Photometrically Using Optical Fibers and Comparison of the Method with Ordinary Techniques," *J. Memb. Sci.*, **88**, 159 (1994).

Kaufmann, T. G., and E. F. Leonard, "Studies of Intramembrane Transport: A Phenomenological Approach," *AIChE J.*, **14**, 110 (1968).

Klein, E., F. F. Holland, A. Lebeouf, A. Donnaud, and J. K. Smith, "Transport and Mechanical Properties of Hemodialysis Hollow Fibers," *J. Memb. Sci.*, **1**, 371 (1976).

Klein, E., F. F. Holland, and R. P. Wendt, "Membrane and Material Evaluation," *Ann. Prog. Rep., NIH Jan.*, 21, NTIS Access No. PB275 463/8 WV (1977).

Klein, E., F. F. Holland, and K. Eberle, "Rejection of Solutes by Hemofiltration Membranes," *ASAIO J.*, **1**, 15 (1978).

Klein, E., F. F. Holland, and K. Eberle, "Comparison of Experimental and Calculated Permeability and Rejection Coefficient for Hemodialysis Membranes," *J. Memb. Sci.*, **5**, 173 (1979).

Kokubo, K., T. Yakushiji, and K. Sakai, "Diffusive Permeability of Asymmetrical Polysulfone Dialysis Membranes with Pore Size and Pore Size Distribution of Their Skin and Supporting Layers," *Artif. Organs Today*, **5**, 185 (1996).

Mackie, J. S., and P. Meares, "The Diffusion of Electrolytes in a Cation-Exchange Resin Membrane," *Proc. Roy. Soc. Ser. A.*, **232**, 498 (1955).

Mochizuki, S., and A. L. Zydney, "Theoretical Analysis of Pore Size Distribution Effects on Membrane Transport," *J. Memb. Sci.*, **82**, 211 (1993).

Nakao, S., and S. Kimura, "Analysis of Solutes Rejection in Ultrafiltration," *J. Chem. Eng. Jpn.*, **14**, 32 (1981).

Nakao, S., and S. Kimura, "Models of Membrane Transport Phenomena and Their Application for Ultrafiltration," *J. Chem. Eng. Jpn.*, **15**, 200 (1982).

Ohmura, T., T. Tatsuguchi, J. Nishikido, T. Yamamoto, F. Fushimi, O. Nishida, and K. Sakai, "A New Method of Determining the Solute Permeability of Hollow-Fiber Dialysis Membranes by Means of Laser Lights Travelling Along Optic Fibers," *Trans. Am. Soc. Artif. Int. Organs*, **35**, 601 (1989).

Opong, W. S., and A. L. Zydney, "Diffusive and Convective Protein Transport Through Asymmetric Membranes," *AIChE J.*, **37**, 1497 (1991).

Pappenheimer, J. R., E. M. Renkin, and L. M. Borrero, "Filtration, Diffusion and Molecular Sieving Through Peripheral Capillary Membranes—A Contribution to the Pore Theory of Capillary Permeability," *Am. J. Physiol.*, **167**, 13 (1951).

Polson, A., "Some Aspects of Diffusion in Solution and a Definition of a Colloidal Particle," *J. Phys. Colloid and Chem.*, **54**, 649 (1950).

Quinn, J. A., J. L. Anderson, W. S. Ho, and W. J. Petzny, "Model Pores of Molecular Dimension. The Preparation and Characterization of Track-Etched Membranes," *Biophys. J.*, **12**, 990 (1972).

Robertson, B. C., and A. L. Zydney, "Hindered Protein Diffusion in Asymmetric Ultrafiltration Membranes with Highly Constricted Pores," *J. Memb. Sci.*, **49**, 287 (1990).

Sakai, K., R. Mimura, K. Ozawa, and S. Takesawa, "A Physicochemical Determination of Pore Diameter of Small Tubular Membranes in Currently-Utilized Hemodialyzers," *Trans. Eur. Conf. on Biomaterials*, p. 63 (1985).

Sakai, K., S. Takezawa, R. Mimura, and H. Ohashi, "Structural Analysis of Hollow Fiber Dialysis Membranes for Clinical Use," *J. Chem. Eng. Jpn.*, **20**, 351 (1987).

Sakai, K., S. Takesawa, R. Mimura, and H. Ohashi, "Determination of Pore Radius for Hollow-Fiber Dialysis Membranes Using Tritium-Labeled Water," *J. Chem. Eng. Jpn.*, **21**, 207 (1988).

Spiegler, K. S., "Transport Processes in Ionic Membranes," *Trans. Farad. Soc.*, **54**, 1408 (1958).

Stevenson, J. F., "Unsteady Mass Transfer in a Long Composite Cylinder with Interfacial Resistances," *AIChE J.*, **20**, 461 (1974).

Tsapuik, E. A., M. T. Bryk, V. M. Kochkodan, and E. E. Danilenko, "Separation of Aqueous Solution of Nonionic Solutes by Ultrafiltration," *J. Memb. Sci.*, **48**, 1 (1990).

Verniory, A., R. Dubois, P. Decoodt, J. P. Gassee, and P. P. Lambert, "Measurement of the Permeability of Biological Membranes, Application to the Glomerular Wall," *J. Gen. Physiol.*, **62**, 489 (1973).

Wendt, R. P., and E. A. Mason, "Effect of Heteroporosity on Membrane Rejection Coefficients," *J. Memb. Sci.*, **8**, 69 (1981).

Manuscript received Mar. 13, 1998, and revision received Sept. 21, 1998.